# LLDPE/TiO$_2$ nanocomposites produced from different crystallite sizes of TiO$_2$ via *in situ* polymerization

CHAICHANA Ekrachan[1], PATHOMSAP Somsakun[2], MEKASUWANDUMRONG Okorn[3], PANPRANOT Joongjai[2], SHOTIPRUK Artiwan[2] & JONGSOMJIT Bunjerd[2*]

[1] *Chemistry Program, Faculty of Science and Technology, Nakhon Pathom Rajabhat University, Nakhon Pathom 73000, Thailand;*

[2] *Faculty of Engineering, Department of Chemical Engineering, Center of Excellence on Catalysis and Catalytic Reaction Engineering, Chulalongkorn University, Bangkok 10330, Thailand;*

[3] *Faculty of Engineering and Industrial Technology, Silapakorn University, Nakhon Prathom 26000, Thailand*

Nano-TiO$_2$ particles with a range of crystallite sizes were synthesized by a conventional sol-gel method, and then used as nanoparticle substrates in the synthesis of LLDPE/TiO$_2$ nanocomposites via *in situ* polymerization of ethylene/1-hexene with zirconocene/MMAO catalyst. It was found that the size of the nano-TiO$_2$ crystallite nanoparticles can influence the catalytic activity in the polymerization system. The larger nano-TiO$_2$ crystallites provided better catalytic activity in the polymerization system due to more space for monomer attack. In addition, by thermo-gravimetric analysis, it can be seen that the larger nano-TiO$_2$ crystallites also exhibited lower interaction with available MMAO. Consequently, the MMAO reacted more efficiently with the zirconocene catalyst during the activation process, and enhanced polymerization catalysis. All the polymer nanocomposites products did not have well defined melting temperature indicating non-crystalline polymers. This is due to the high amount of hexene incorporation (based on $^{13}$C NMR). The difference in crystallite sizes of the nano-TiO$_2$ also affected how 1-hexene became incorporated into the polymer nanocomposites. The smaller crystallite size of nano-TiO$_2$ allowed greater 1-hexene incorporation due to depression of the reactivity of the ethylene. The contribution of this work helps develop a better understanding of the role of nano-TiO$_2$ in the catalytic activity of the polymerization system and in the microstructure of the polymer composite product. However, this study only considers work on the laboratory scale, so for commercial application of these results, it is necessary to scale up the polymerization process. It is only at this stage, that other physical properties, such as the mechanical properties of these materials can be sensibly determined.

**nanocrystal, polymer nanocomposite, polyethylene, sol-gel, TiO$_2$**

Polymer nanocomposites are composed of a polymer matrix and a discontinuous phase nanomaterial, giving bulk properties better than the polymer on its own. Examples of the advantages offered by nanomaterials over conventional composite material are high optical transparency and a high degree of interfacial interaction due to small particle size and high surface area [1]. Therefore, studies of the synthesis and use (as a nanoparticle/reinforcement) of nanomaterials are of great interest. The most commonly used composite nanomaterials are SiO$_2$ [2–4], TiO$_2$ [5–8], Al$_2$O$_3$ [9,10], and ZrO$_2$ [11,12]. Although nano-silica (nano-SiO$_2$) is considered to be the most widely used material, others are also becoming commercially available, especially nano-titania (nano-TiO$_2$), which has particularly, interesting photocatalytic properties and unique optical properties (high refractive index and strong UV light absorption) [13]. The use of nano-TiO$_2$ in nanocomposites has previously been investigated by our group [14,15]. These studies showed that

*Corresponding author (email: bunjerd.j@chula.ac.th)

nano-TiO$_2$ can be employed in preparing LLDPE nanocomposites (by *in situ* polymerization of ethylene and 1-hexene) with a good particulate distribution through the polymer matrix. The proportions of the titania phases (anatase and rutile) affect catalytic activity in the polymerization system and hence the properties of the nanocomposite product. Differences in shape (spheroid for anatase and acicular for rutile) could be the reason for this. However, careful consideration of the nature of the two different phases of nano-TiO$_2$ shows that, besides the shapes difference, they also have different crystallite sizes. Therefore, to develop a better understanding on the role of nano-TiO$_2$ in nanocomposites, we need to understand the role of the sizes of nano-TiO$_2$ crystallites. The synthesis of controlled crystallite size nano-TiO$_2$ can be performed with a conventional sol-gel method [16]. This technique allows the control of certain of the nanosolid parameters by setting the parameters before gelation takes place and consequently allowing the preparation of tailor-made nanomaterials [17]. Therefore, once the relation between crystallite size and the properties of a polymer nanocomposite is established, a polymer nanocomposite can be synthesized with tailor-made properties. To retain the qualities associated with nanoscale inclusions during manufacture of the nanocomposite, *in situ* polymerization techniques (a proven method to provide good dispersion of nano-sized metal oxides into polyolefins [18]) were used. Typically, *in situ* polymerization involves the following steps: (1) preparation of a supported catalyst (immobilizing the catalytic species onto a particulate), (2) *in situ* olefin polymerization using the supported catalyst in a suspension polymerization system, and (3) production of nanocomposites with a well dispersed nanomaterial phase [19].

We have prepared nano-TiO$_2$ particles with controlled variation in crystallite size by a conventional sol-gel method. These nanoparticles were employed as composite reinforcements and as supporting material for the zirconocene/MMAO catalyzed *in situ* polymerization of ethylene and 1-hexene. The subject of this paper is how the catalytic activity and properties of the LLDPE/TiO$_2$ nanocomposites vary with nano-titania crystallite size.

# 1    Materials and methods

## 1.1    Chemicals

All the chemicals reactions and the polymerization were performed under an argon atmosphere using a glove box and/or Schlenk techniques. Titanium isopropoxide (99.999%) was purchased from the Aldrich Chemical Company, Inc. Ethanol (anhydrous) was also purchased from Aldrich Chemical Company, Inc. Toluene was dried over dehydrated CaCl$_2$ and distilled over sodium/benzophenone before use. The rac-ethylenebis (indenyl) zirconium dichloride

(rac-Et[Ind]$_2$ZrCl$_2$) was obtained from the Aldrich Chemical Company, Inc. Modified methylaluminoxane (MMAO) in hexane was donated by Tosoh (Akzo, Japan). Trimethylaluminum (TMA, 2 mol/L in toluene) was supplied by Nippon Aluminum Alkyls, Ltd., Japan. Ultrahigh purity argon was purchased from Thai Industrial Gas Co., Ltd., and further purified by passing it through columns that were packed with BASF catalyst R3-11G (molecular-sieved to 3 Å), sodium hydroxide (NaOH), and phosphorus pentaoxide (P$_2$O$_5$) to remove traces of oxygen and moisture. Ethylene gas (99.96%) was donated by the National Petrochemical Co., Ltd., Thailand. 1-Hexene (99%, $d = 0.673$ g/mL) was purchased from Aldrich Chemical Company, Inc.

## 1.2    Preparation of nano-TiO$_2$ nanoparticles

Nano-TiO$_2$ nanoparticles were synthesized via the sol-gel method using Ti(i-OPr)$_4$ in a solution of water and methanol according to the method described by Wang and Ying [16]. The molar ratio of water∶alkoxide varied between 4, 16 and 80 to vary the nano-TiO$_2$ crystallite size.

## 1.3    *In situ* polymerization reaction

The ethylene and 1-hexene copolymerization reaction was carried out in a 100 mL semi-batch stainless steel autoclave reactor equipped with a magnetic stirrer. Using a glove box, the desired amount of the nano-TiO$_2$ was placed into the reactor and magnetically stirred with 1.14 mL of MMAO for 30 min. Then, toluene was introduced into the reactor to a total volume of 30 mL. Separately, the desired amount of Et(Ind)$_2$ZrCl$_2$ ($5 \times 10^{-5}$ mol/L) and TMA ([Al]$_{TMA}$/[Zr]$_{cat}$ = 2500) was mixed and stirred in a 5-min aging process at room temperature. This mixture was then injected into the reactor. The reactor was frozen in liquid nitrogen to stop the reaction, and then injected with 0.018 mol of 1-hexene. The reactor was evacuated to remove the argon atmosphere, and was then heated up to the polymerization temperature (70°C). To start the polymerization reaction, 0.018 mol of ethylene (at 6 psi gauge) was fed into the reactor containing the 1-hexene and catalyst mixtures. After the ethylene was totally consumed, the reaction was terminated by the addition of acidic methanol, and then stirred for 30 min. The copolymer product (white powder) was filtered, washed with methanol and dried at room temperature.

## 1.4    Characterization of nano-TiO$_2$ nanoparticles

(1) X-ray diffraction (XRD).    XRD was performed to determine the bulk crystalline phases of the samples using a Siemens D-5000 X-ray diffractometer with CuKα ($k = 1.54439$ Å). The spectra were scanned at a rate of 2.4°/min in the range $2\theta = 20°$–$80°$.

(2) BET surface area.    Surface area measurement was

carried out by low temperature nitrogen adsorption in a Micromeritic ChemiSorb 2750 system.

(3) Scanning electron microscopy (SEM).   SEM was used to investigate the morphology of the nano-TiO$_2$. A JEOL mode JSM-5800 LV scanning microscope was employed.

(4) Transmission electron microscopy (TEM). TEM was used to determine the shape and crystalline size of the nano-TiO$_2$. Samples were dispersed in ethanol prior to TEM measurement using a JEOL JEM-2010.

(5) Thermal gravimetric analysis (TGA).   TGA was performed using a TA Instruments SDT Q-600 analyzer. Samples of 10–20 mg were examined at a temperature ramping from 25 to 600°C at 2°C/min. The carrier gas was N$_2$ UHP.

## 1.5   Polymer characterization

(1) Differential scanning calorimetry (DSC).   DSC was used to determine the melting temperature of ethylene/ 1-hexene copolymer products with a Perkin-Elmer Diamond DSC. The analyses were performed at a heating rate of 20°C/min in the temperature range of 50–150°C.

(2) [13]Carbon nuclear magnetic resonance (^{13}C NMR).   ^{13}C NMR spectroscopy was used to determine 1-hexene incorporation and copolymer microstructure. Each sample solution was prepared by dissolving 50 mg of copolymer in 1,2-dichlorobenzene and CDCl$_3$. The ^{13}C NMR spectra were taken at 100°C using a Bruker Avance II 400 operating at 100 MHz with an acquisition time of 1.5 s and a delay time of 4 s.

## 2   Result and discussion

### 2.1   Characterization of nanoparticles

A range of nano-TiO$_2$ nanoparticles, prepared by the sol-gel method by varying the water to alkoxide ratio, were investigated by XRD and the BET method to obtain their crystal structures and specific surface areas. From Figure 1, it can be seen that all the nano-TiO$_2$ nanoparticles exhibited XRD peaks at 25°, 37°, 48°, 55°, 56°, 62°, 69°, 71°, and 75° assigned to anatase TiO$_2$. The crystallite sizes of the nanoparticles can also be measured from their XRD peaks using the Sherrer equation, as shown in Table 1 (along with the surface areas). The TiO$_2$ samples are labeled by crystallite size. It was found that the crystallite sizes of nano-TiO$_2$ increased as the water:alkoxide ratio decreased. This is because the water:alkoxide ratio determines the nature of the sol-gel chemistry and the structural characteristics of the hydrolyzed gel. High water:alkoxide ratios in the reaction medium ensure a more complete hydrolysis of alkoxides, favoring nucleation over particle growth, thus, reducing crystallite sizes of the nano-TiO$_2$ product [16]. As expected, the specific surface area of the nano-TiO$_2$ decreased as crystallite size increased.
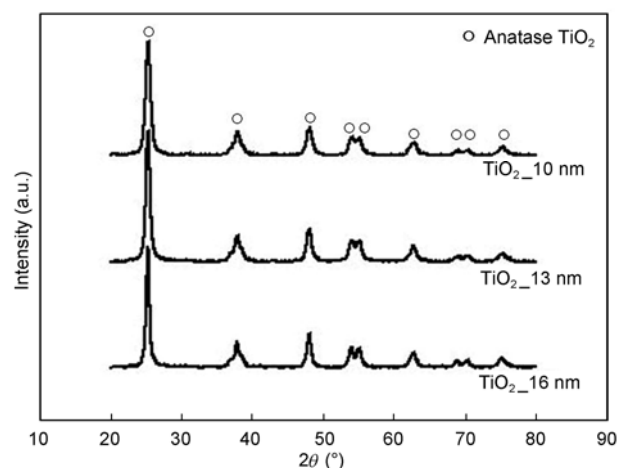


**Figure 1**   XRD patterns of nano-TiO$_2$ nanoparticles with different crystallite sizes.

**Table 1**   Properties of nano-TiO$_2$ nanoparticles prepared with a range of water:alkoxide ratios

| Sample | Water:alkoxide ratio | Average crystallite size[a] (nm) | BET surface area (m$^2$/g) |
|---|---|---|---|
| TiO$_2$_10 nm | 80 | 10 | 79 |
| TiO$_2$_13 nm | 16 | 13 | 58 |
| TiO$_2$_16 nm | 4 | 16 | 48 |

a) Determined by XRD and based on the Sherrer equation.

Variations in the morphology of the nano-TiO$_2$ nanoparticles observed by SEM are shown in Figure 2. It can be seen that pristine nano-TiO$_2$ tends to agglomerate. However, these agglomerations would be reduced in size as primary particles under the specific conditions of polymerization by the hydraulic force exerted by the growing polymer when the nanoparticles are used in polymerization [20,21]. When comparing the three types of nano-TiO$_2$, it can be seen that the smaller crystallite particles agglomerate more. The agglomerated particles may affect the fragmentation during polymerization and consequently the catalytic activity of the system.

These SEM images do not provide sufficient detail of the nanomaterial structure and morphology. As can be seen in Figure 2, the sizes of particles in the images were not the same as the sizes measured by XRD. Therefore, higher resolution TEM was used to provide further details of the nano-TiO$_2$ particles. The TEM images in Figure 3 show that the aggregated primary particles were somewhat spherical in nature. All the nano-TiO$_2$ particles had the sizes in close agreement with those obtained from the XRD measurement and the Sherrer equation. As particle size varied, no change in shape was observed.

### 2.2   Catalytic activity
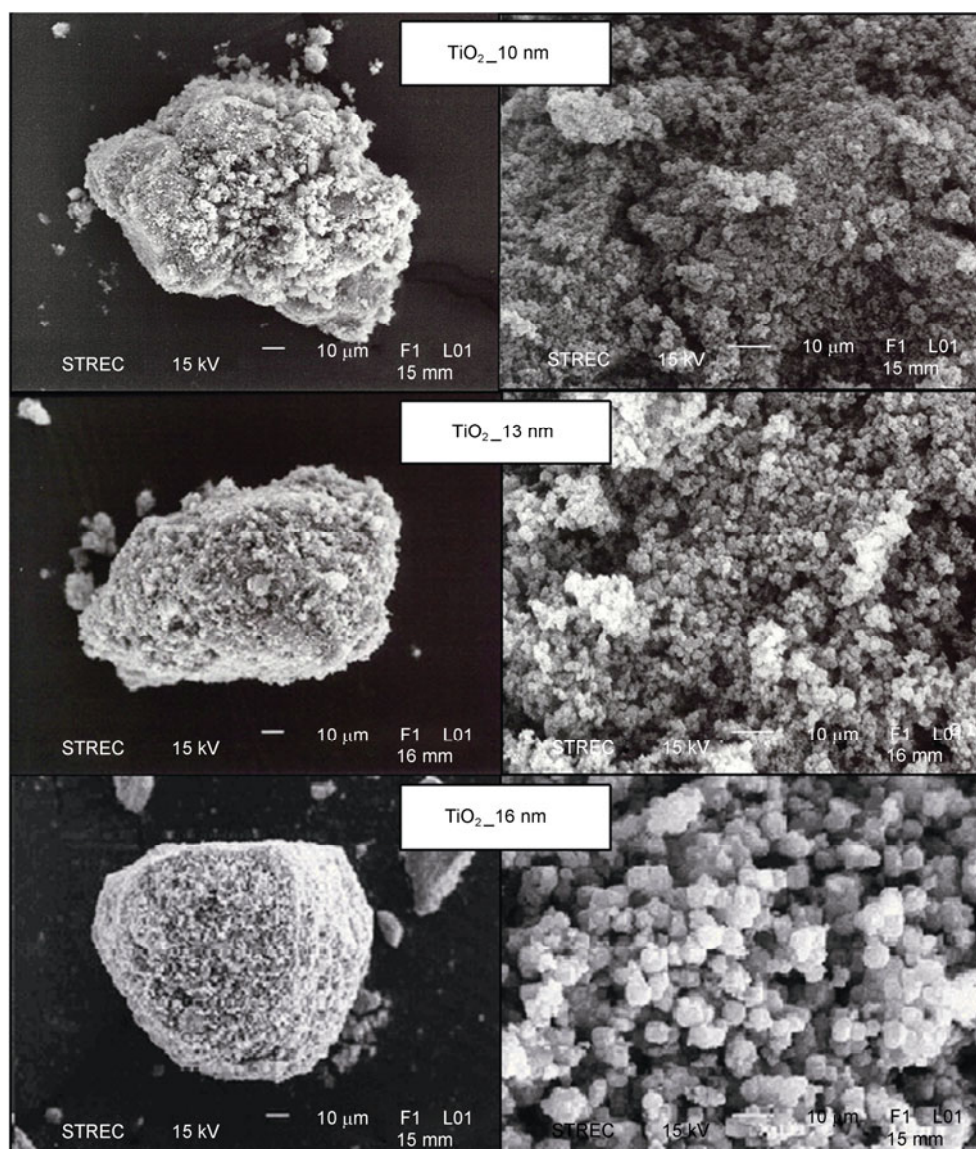
How catalytic activity of the polymerization systems varied

**Figure 2**    SEM micrographs of nano-TiO$_2$ nanoparticles with different crystallite sizes.

with nano-TiO$_2$ crystallite size is shown in Table 2.

It was found that catalytic activities increased with increased crystallite sizes (or primary particle size) of the nano-TiO$_2$ nanoparticles. This result accords with our previous work including that the larger sizes of nano-SiO$_2$ nanoparticles gave higher catalytic activity [22]. This is because the larger particles render less steric hindrance and also afford more space for the monomer to attack compared with the smaller particles, leading to the higher catalytic activity observed. Although nano-SiO$_2$ nanoparticles were used in this work, a similar trend of activity was observed. This means that in both studies the size of the nanoparticles is one of the crucial parameters that can control the catalytic activities of the polymerization system.

Besides the clear difference in crystallite sizes that was observed in the three types of nano-TiO$_2$ nanoparticles,

other properties also vary, and must therefore be considered. As seen in Table 1, increasing the surface areas of the nano-TiO$_2$ nanoparticles (which decrease with increased crystallite size) adversely affected polymerization. This result is counterintuitive, as with the supporting materials, a higher surface area should provide better distribution of catalytically active centers throughout the particle, offering easy access for the monomer and consequently enhancing a catalytic activity [23]. Therefore, in this case, the specific surface area of the nanoparticles may affect the activity of the system less than the crystallite size, but the effect of crystallite size is more pronounced. It is known that crystal properties can play an important role in determining properties of the particles including adsorption and reactivity [24]. Both adsorption and reactivity of the nanoparticles can influence the activity of the polymerization system both as
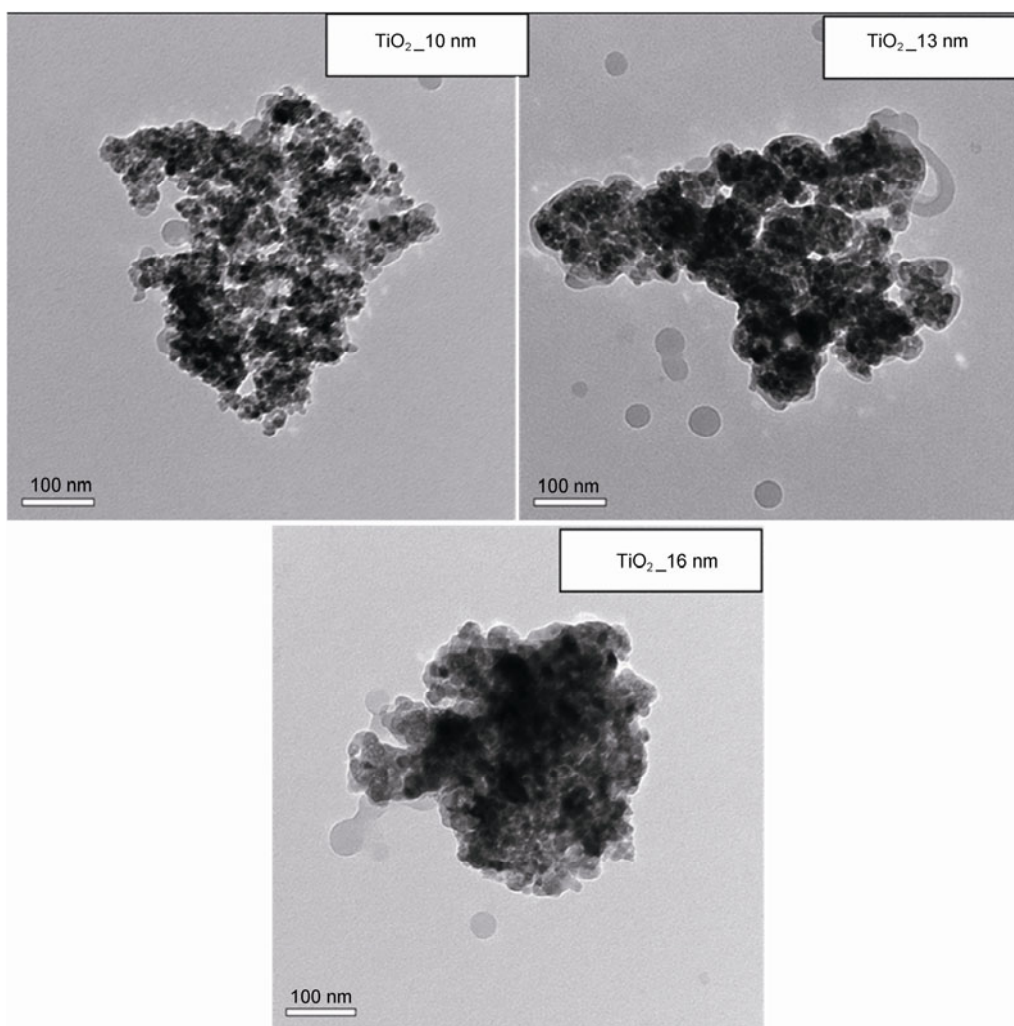
**Figure 3** TEM micrographs of nano-TiO$_2$ nanoparticles with different crystallite sizes.

**Table 2** Polymerization activities of LLDPE/TiO$_2$ nanocomposites

| Sample | Polymerization time [a] (s) | Polymerization yield[b] (g) | Catalytic activity (kg polymer/mol Zr h) |
|---|---|---|---|
| TiO$_2$_10 nm | 103 | 1.30 | 30296 |
| TiO$_2$_13 nm | 115 | 1.54 | 32112 |
| TiO$_2$_16 nm | 102 | 1.44 | 33922 |

a) Period of time used for the total 0.018 mol of ethylene to be consumed; b) measurement at polymerization temperature of 70°C, [ethylene] = 0.018 mol, $[Al]_{MMAO}/[Zr] = 1135$, $[Al]_{TMA}/[Zr]_{cat} = 2500$, in toluene with total volume = 30 mL, and $[Zr]_{cat} = 5 \times 10^{-5}$ mol/L.

nanoparticles and as supporting materials. Particularly, it should be noted that the adsorption characteristics of the nanoparticles are very important.

To clarify this relationship between the adsorption and activity, the polymerization system must be considered in detail. In the first stage, MMAO was thought to adsorb onto the surface of the nanoparticles through covalent bonding of oxygen and aluminium (O$_{nanoparticles}$−Al$_{MMAO}$) and some might be adsorbed onto the surface nanoparticles by physi-

cal force without the formation of a chemical bond. The MMAO on the nanoparticles then activates the metallocene catalyst. The final stage is that the active catalysts polymerized the ethylene and 1-hexene to obtain the LLDPE/nanocomposites product. So, MMAO as proposed has many functions in the catalytic system such as an alkylating and a reducing agent, a stabilizer for a cationic metallocene alkyl and/or the counter-ion, a scavenger for the metallocene catalytic system, and a buffer to prevent the formation of ZrCH$_2$CH$_2$Zr species (formed via a bimolecular process causing catalyst deactivation) [14]. MMAO performs the functions mentioned and is still present on the nanoparticles, the adsorption characteristics of the interaction between nanoparticles and MMAO, then directly affects the consequent catalytic activity and the performance of the whole system [25]. Therefore, this interaction must be investigated to provide a reasonable explanation for the observed results. One of the most powerful techniques that can quantify the degree of interaction is TGA. TGA can provide useful information in term of weight loss and temperature at which

the weight is lost. Lower weight loss can be evidence of a stronger interaction between the adsorbed species (MMAO) and the nanoparticles. The TGA profile of [Al]$_{MMAO}$ with different crystallite size nano-TiO$_2$ nanoparticles is shown in Figure 4.

It was found that the weight loss of [Al]$_{MMAO}$ on each type of nano-TiO$_2$ nanoparticles was as follows: TiO$_2$_16 nm (17%) > TiO$_2$_13 nm (16%) > TiO$_2$_10 nm (13%). This indicated that the [Al]$_{MMAO}$ present on the TiO$_2$_10 nm nanoparticle exhibited the strongest interaction of all the samples. Thus, the interaction of MMAO on the nanoparticles is clearly related to the crystallite size, with smaller nanoparticles exhibited a stronger interaction. This result also supported the earlier assumption that adsorption characteristics can be influenced by crystal structure. In addition, the strong interaction may not only persist between the nanoparticles and MMAO, but also between the nanoparticles themselves. When considering the morphologies of nano-TiO$_2$ shown in Figure 2, we conclude that the tighter agglomeration of the smaller particles may be derived from this stronger interaction.

The degree of interaction between MMAO and nanoparticles indicated by TGA measurement, adversely affects catalytic activity. This is probably due to the stronger interaction, which results in hindrance of the MMAO bound to the support, in reacting with the metallocene catalyst during the activation processes. This leads to lower catalytic activity for polymerization. In addition, the stronger interaction
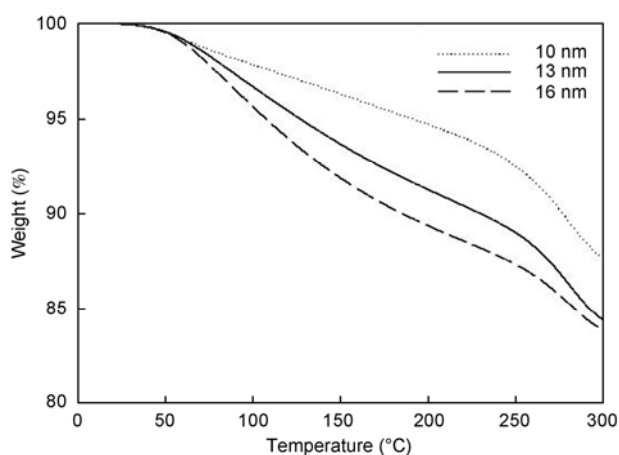
which caused the tighter agglomeration of the particles could result in less particle fragmentation and thus, less monomer access to the catalytically active sites, so decreasing catalytic activity. Therefore, we conclude that the smaller crystallite nano-TiO$_2$ nanoparticles have lower catalytic activity due to stronger inter-particle interactions.

### 2.3    Characterization of LLDPE/TiO$_2$ nanocomposites

The LLDPE/TiO$_2$ nanocomposites were further characterized by DSC and $^{13}$C NMR techniques to investigate how the different crystallite sizes in the nanoparticles affect the properties of the polymers.

Sharp melting temperatures ($T_m$) are not seen in the DSC traces taken from the LLDPE/TiO$_2$ nanocomposites (not shown) indicating the non-crystalline nature of the polymers. This contrasts with Lingaraju et al. [26], where crystallite inclusions in a non-crystalline material transformed the material into the crystalline form. However, there was a major difference between two systems due to the polymer matrix. Lingaraju et al. [26] used an epoxy as the polymer matrix while this study used LLDPE as polymer matrix. In general, the crystallinity of polymer composites can be controlled by the introduction of particles because they act as nucleating agents, becoming a starting point for the crystallization process [27]. For an epoxy polymer, the crystal can form rapidly when it solidifies (at about 50°C) and introduction of nanoparticles can accelerate the crystallization process, therefore significantly enhancing the degree of crystallinity. However, for LLDPE (copolymer of ethylene and 1-olefins), there is another factor greatly influencing crystallinity, namely, the proportion of olefins (1-hexene) in the copolymer chain [28]. By increasing the co-monomer content, the crystallinity of LLDPE is decreased. Therefore, although a high amount of nanoparticles were present in the polymer composites; the composites would still not be highly crystalline if there was too much 1-hexene incorporation. Hence, a technique to investigate the amount of 1-hexene in the polymer composites should be employed to support the claim that non-crystallinity resulted from a high level of 1-hexene incorporation.

A quantitative analysis of the triad distribution in the composites can be obtained from characteristics of the $^{13}$C NMR spectra (not shown) of the polymer composites by calculation (Randall [29]) as shown in Table 3.



**Figure 4**   The TGA profile of [Al]$_{MMAO}$ with different crystallite size nano-TiO$_2$ nanoparticles.

**Table 3**   Triad distribution, reactivity of ethylene and 1-hexene of LLDPE/TiO$_2$ nanocomposites obtained from $^{13}$C NMR analysis

| Sample | Triad distribution of copolymer[a] | | | | | | Incorporation (mol%) | | Reactivity[b] | | |
|---|---|---|---|---|---|---|---|---|---|---|---|
| | HHH | EHH | EHE | EEE | HEH | HEE | Ethylene | 1-Hexene | $r_E$ | $r_H$ | $r_E r_H$ |
| TiO$_2$_10 nm | 0.000 | 0.377 | 0.086 | 0.359 | 0.028 | 0.150 | 53.7 | 46.3 | 0.253 | 1.164 | 0.295 |
| TiO$_2$_13 nm | 0.000 | 0.221 | 0.109 | 0.398 | 0.089 | 0.182 | 67.0 | 33.0 | 0.684 | 0.334 | 0.228 |
| TiO$_2$_16 nm | 0.000 | 0.144 | 0.131 | 0.438 | 0.086 | 0.200 | 72.4 | 27.6 | 1.421 | 0.105 | 0.150 |

a) Calculated by Randall's [29] method; b) relative co-monomer reactivities ($r_E$ for ethylene and $r_H$ for 1-hexene) calculated by $r_E$ = [EE]/[EC]X, $r_H$ = 2X[CC]/[EC], [EE] = [EEE] + 0.5[CEE], [CC] = [CCC] + 0.5[ECC], [EC] = [CEC] + 0.5[CEE] + [ECE] + 0.5[ECC].

It can be seen that the amounts of 1-hexene incorporation (converted from the triad distribution) in the entire polymer composites were greater than 27 mol%. These values are too high for LLDPE to have a sharp melting temperature. In our previous study, with similar polymerization conditions [14], it was also found that the polymers had no sharp melting temperature when the amount of the co-monomer incorporation rose above 20 mol%. Therefore, this supports the idea that non-crystalline polymer composites result from the high amount of hexene incorporation and the introduction of nano-TiO$_2$ (nucleating material) cannot improve the crystallinity of the composites no matter what the nano-TiO$_2$ crystallite sizes are.

Besides the co-monomer content, the reactivity of ethylene ($r_E$) and 1-hexene ($r_H$), and the product of both ($r_E r_H$) were also calculated using the triad distribution, as shown in Table 3. The value of $r_E r_H$ can identify types of co-monomer by $r_E r_H > 1$ indicating a block copolymer structure and $r_E r_H < 1$ indicating an alternating copolymer structure. Therefore, from the values in Table 3, all the polymer composites were alternating copolymers. Hung et al. [30] note that the disadvantage of alternating copolymer is that a polymer with a highly alternating sequence distribution does not exhibit a sharp melting point. This is because the co-monomers in their chain are distributed moderately well along the backbone, and shortens the average backbone sequence length for crystallization and therefore lowers the crystallinity. Hence, the sequence distribution could be one of the reasons for the non-crytalline form of the obtained composites. The decrease in $r_E$ with nano-TiO$_2$ crystallite size is observed. In fact, depressed reactivity of the monomer (ethylene) in a supported system was observed by Xu et al. [31]. This means that for this system, the smaller crystallite size nanoparticles have a stronger effect in the supported system on the ethylene reactivity. This may be due to the smaller crystallite size nanoparticle occupying more of the bulk reaction zone (leaving less space) during polymerization, and then having greater effect on the ethylene reactivity.

However, when contrasted with ethylene reactivities, the reactivities of 1-hexene increase with decrease in nano-TiO$_2$ crystallite size. This is because the greater depression of ethylene in the smaller crystallite size nanoparticles should lead to higher 1-hexene reactivity. In fact, the different reactivities of ethylene and 1-hexene caused by variation in crystallite size support that observation that crystallite size is a crucial property to consider when designing a production system for LLDPE/TiO$_2$ nanocomposites.

These findings help develop a better understanding of the role of nano-TiO$_2$ in the catalytic activity of the polymerization system and in the microstructure of the polymer nanocomposite product. This paper only considers work on the laboratory scale, so for commercial application of these results, it is necessary to scale up the polymerization process. It is only at this stage that other physical properties, such as the mechanical properties of these materials can be sensibly determined.

# 3    Conclusions

It can be concluded from this study that the variation in the size of nano-TiO$_2$ crystallites significantly affects both catalytic activities for the polymerization system and the characteristic properties of the polymer composite product. Therefore, by controlling the crystallite sizes of nano-TiO$_2$ nanoparticles, the properties of the polymer nanocomposites can be controlled. Larger nano-TiO$_2$ crystallite sizes provide better polymerization catalysis due to less steric hindrance, more space for monomer attack and lower interaction with MMAO (as indicated by the TGA results). None of the polymer nanocomposites exhibited a sharp melting temperature indicating the non-crystalline nature of the polymers, even though inclusions of crystallite material were present. This was because of the high amount of 1-hexene incorporated in the polymer composites. It was also found that the smaller crystallite size of nano-TiO$_2$ allowed greater 1-hexene incorporation due to depression of the reactivity of the ethylene.

1    Jordan J, Jacob K I, Tannenbaum R, et al. Experimental trends in polymer nanocomposites—A review. Mater Sci Eng A, 2005, 293: 1–11

2    Zou H, Wu S, Shen J. Polymer/silica nanocomposites: Preparation, characterization, propertles, and applications. Chem Rev, 2008, 108: 3893–3957

3    Kontou E, Niaounakis M. Thermo-mechanical properties of LLDPE/SiO$_2$ nanocomposites. Polymer, 2006, 47: 1267–1280

4    Li K T, Dai C L, Kuo C W. Ethylene polymerization over a nano-sized silica supported Cp$_2$ZrCl$_2$/MAO catalyst. Catal Commun, 2007, 8: 1209–1213

5    Chen X D, Wang Z, Liao Z F, et al. Roles of anatase and rutile TiO$_2$ nanoparticles in photooxidation of polyurethane. Polym Test, 2007, 26: 202–208

6    Nussbaumer R J, Caseri W R, Tervoort P T. Polymer-TiO$_2$ nanocomposites: A route towards visually transparent broadband UV filters and high refractive index materials. Macromol Mater Eng, 2003, 288: 44–49

7    de Fátima V, Marques M, da Silva O, et al. Ethylene polymerization catalyzed by metallocene supported on mesoporous materials. Polym Bull, 2008, 61: 415–423

8    Zhang Q, He Y Q, Chen X G, et al. Structure and photocatalytic properties of TiO$_2$-graphene oxide intercalated composite. Chin Sci Bull, 2011, 56: 331–339

9    Kuo M C, Tsai C M, Huang J C, et al. PEEK composites reinforced by nano-sized SiO$_2$ and Al$_2$O$_3$ particulates. Mater Chem Phys, 2005, 90: 185–195

10    Pitukmanorom P, Ying J Y. Selective catalytic reduction of nitric oxide by propene over In$_2$O$_3$-Ga$_2$O$_3$/Al$_2$O$_3$ nanocomposites. Nano Today, 2009, 4: 220–226

11    Sagmeister M, Brossmann U, List E J W, et al. Synthesis and optical properties of organic semiconductor: Zirconia nanocomposites. J Nanopart Res, 2010, 12: 2541–2551

12 Liang R, Deng M, Cui S, et al. Direct electrochemistry and electrocatalysis of myoglobin immobilized on zirconia/multi-walled carbon nanotube nanocomposite. Mater Res Bull, 2010, 45: 1855–1860

13 Yang D, Ni X, Chen W, et al. The observation of photo-Kolbe reaction as a novel pathway to initiate photocatalytic polymerization over oxide semiconductor nanoparticles. J Photochem Photobiol B, 2008, 195: 323–329

14 Owpradit W, Jongsomjit B. A comparative study on synthesis of LLDPE/TiO₂ nanocomposites using different TiO₂ by *in situ* polymerization with zirconocene/dMMAO catalyst. Mater Chem Phys, 2008, 112: 954–961

15 Owpradit W, Mekasuwandumrong O, Panpranot J, et al. Synthesis of LLDPE/TiO₂ nanocomposites by *in situ* polymerization with zirconocene/dMMAO catalyst: Effect of [Al]/[Zr] ratios and TiO₂ phases. Polym Bull, 2011, 66: 479–490

16 Wang C C, Ying J Y. Sol-gel synthesis and hydrothermal processing of anatase and rutile titania nanocrytals. Chem Mater, 1999, 11: 3113–3120

17 Dominguez A M, Zarate A, Quijada R, et al. Sol-gel iron complex catalysts supported on TiO₂ for ethylene polymerization. J Mol Catal A: Chem, 2004, 207: 155–161

18 Guo N, DiBenedetto S A, Kwon D K, et al. Supported metallocene catalysis for *in situ* synthesis of high energy density metal oxide nanocomposites. J Am Chem Soc, 2007, 129: 766–767

19 Qin Y, Dong J. Preparation of nano-compounded polyolefin materials through *in situ* polymerization technique: Status quo and future prospects. Chin Sci Bull, 2009, 54: 38–45

20 Fink G, Tesche B, Korber F, et al. The particle forming process of SiO₂-supported metallocene catalysts. Macromol Symp, 2001, 173: 77–87

21 Goretzki R, Fink G, Tesche B, et al. Unusual ethylene polymerization results with metallocene catalysts supported on silica. J Polym Sci Part A: Polym Chem, 1999, 37: 677–682

22 Chaichana E, Jongsomjit B, Praserthdam P. Effect of nano-SiO₂ particle size on the formation of LLDPE/SiO₂ nanocomposite synthesized via the *in situ* polymerization with metallocene catalyst. Chem Eng Sci, 2007, 62: 899–905

23 Silveira F, Pires G P, Petry C F, et al. Effect of the silica texture on grafting metallocene catalysts. J Mol Catal A-Chem, 2007, 265: 167–176

24 Giammar D E, Maus C J, Xie L. Effects of particle size and crystalline phase on lead adsorption to titanium dioxide nanoparticles. Environ Eng Sci, 2007, 24: 85–95

25 Severn J R, Chadwick J C, Duchateau R, et al. "Bound but not gagged"—Immobilizing single-site α-olefin polymerization catalysts. Chem Rev, 2005, 105: 4073–4147

26 Lingaraju D, Ramji K, Pramila D M, et al. Synthesis, functilization and characterization of silica hybrid nanocomposites. Int J Nanotechnol Appl, 2010, 4: 21–30

27 Luyt A S, Molefi J A, Krump H. Thermal, mechanical and electrical properties of copper powder filled low-density and linear low-density polyethylene composites. Polym Degrad Stab, 2006, 91: 1629–1636

28 Hong H, Zhang Z, Chung T C M, et al. Synthesis of new 1-decene-based LLDPE resins and comparison with the corresponding 1-octene- and 1-hexene-based LLDPE resins. J Polym Sci Part A: Polym Chem, 2007, 45: 639–649

29 Randall J C. A review of high resolution liquid ¹³carbon nuclear magnetic resonance characterizations of ethylene-based polymers. J Macromol Sci R M C, 1989, 29: 201–317

30 Hung J, Cole A P, Waymouth R M. Control of sequence distribution of ethylene copolymers: Influence of comonomer sequence on the melting behavior of ethylene copolymers. Macromolecules, 2003, 36: 2454–2463

31 Xu J T, Zhu Y B, Fan Z Q, et al. Copolymerization of propylene with various higher alpha-olefins using silica-supported rac-Me2Si(lnd)-ZrCl₂. J Polym Sci Pol Chem, 2001, 39: 3294–3303